

# Evaluation of a multi-nodal thermal regulation model for assessment of outdoor thermal comfort: sensitivity to wind speed and solar radiation

Yongxin Xie<sup>a</sup>, Taiyang Huang<sup>a</sup>, Jianong Li<sup>a</sup>, Jianlin Liu<sup>b</sup>, Jianlei Niu<sup>b,\*</sup>, Cheuk Ming MAK<sup>a</sup>, Zhang Lin<sup>c</sup>

<sup>a</sup> Department of Building Services Engineering, The Hong Kong Polytechnic University, Hunghom, Kowloon, Hong Kong

<sup>b</sup> School of Architecture, Design and Planning, The University of Sydney, Australia

<sup>c</sup> Division of Building Science and Technology, The City University of Hong Kong, Kowloon Tong, Hong Kong

\* Corresponding author. Email address: [jianlei.niu@sydney.edu.au](mailto:jianlei.niu@sydney.edu.au), Tel: +61 2 8627 4621

## ABSTRACT:

People's outdoor thermal sensation varies from that indoors. The highly asymmetric solar radiation and transient wind environment are the main causes. The University of California-Berkeley developed a multi-nodal human body thermal regulation model (the UCB model) to predict human thermal sensation and comfort in asymmetric and transient indoor environments. However, few studies compared its predictions with the survey responses outdoors. In this study, subjects' thermal sensations outdoors were surveyed and compared with the UCB model predictions. Meteorological parameters were monitored using a microclimate station, and over a thousand human subjects' thermal sensation levels were surveyed. Results point out that subjects were highly sensitive to the changes in wind speed, especially under low-radiation conditions. However, the UCB model failed to predict such a high sensitivity. Besides, subjects had a higher tolerance to high air temperatures in outdoor environments when the solar radiation was acceptable, but the UCB model over-predicted the TSV (thermal sensation vote) in such conditions. Both the on-site results and the predictions by UCB model showed that subjects were more sensitive to wind speed in hotter environments while they were least sensitive to solar radiation in neutral thermal conditions. This study helps to reveal the potential of a multi-nodal thermal regulation model to address the asymmetric and transient features of outdoor environments and indicates the need to further refine the model for better quantitative prediction of outdoor thermal sensation.

## Keywords:

Outdoor thermal comfort; microclimatic parameters; sensitivity; validation of thermal comfort index

Nomenclature			
$a_k$	Absorption coefficients of the clothed human body in short-wave radiation; suggested value 0.7	$T_b$	Black globe temperature, °C
$\varepsilon_p$	Emissivity of the clothed human body in long-wave radiation; suggested value 0.97	$T_{cl}$	Measured clothing temperature, °C
$\sigma$	Stefan-Boltzmann constant, $5.67 \cdot 10^{-8} \text{ W/m}^2 \text{ K}^4$	$T_g$	Globe temperature, °C
$\frac{A_r}{A_D}$	Ratio of effective radiation area and Dubois surface area; the value is 0.73 for a standing person	$T_{mrt}$	Mean radiant temperature, °C
ANOVA	An analysis of variance	$T_{mrt-i}$	Directional radiant temperature measured by the radiometer, i=1-6
CFD	Computational Fluid Dynamics	$T_{si-i}$	Equivalent surface temperature of the wall in the imaginary room, i=1-6
$F_{i-si}$	Angle factor of the room surface to the differential area	$T_o$	Operative temperature, °C
$h_r$	Radiative heat transfer coefficient, $\text{W/m}^2 \text{ K}$	$T_{skin,i}$	Local skin temperature, °C
$h_c$	Convective heat transfer coefficient, $\text{W/m}^2 \text{ K}$	$\frac{dT_{skin,i}}{dt}$	The derivative of local skin temperature
$K_i$	Short-wave irradiance, $\text{W/m}^2$	$\bar{T}_{skin}$	The mean skin temperature
$L_i$	Long-wave irradiance, $\text{W/m}^2$	$\frac{dT_{core}}{dt}$	The derivative of core temperature
LSD	Least significant difference	UCB model	UC-Berkeley Thermal Comfort Model
MTSV	Mean Thermal Sensation Vote	UTCI	Universal Thermal Climate Index
OUT-SET*	Out-Standard Effective Temperature	$v$	Wind speed, m/s
PET	Physiologically Equivalent Temperature	SET*	Standard Effective Temperature
PMV	Predicted Mean Vote	SPMV	Standard Predicted Mean Vote
TCV	Thermal Comfort Vote	$Sensation_{dynamic}$	Dynamic thermal sensation
TSV	Thermal Sensation Vote	$Sensation_{static}$	Static thermal sensation
RH	Relative humidity, %	$W_i$	Directional dependent weighting factor. With the reference shape of a standing man, 0.06 for the vertical directions and 0.22 for the lateral directions [1]
$T_a$	Air temperature, °C		

35

## 36 1. Introduction

37 The demand for “comfortable” living environments is always a core topic in the area of  
38 building environment [2]. Comfortable indoor environments can be created and  
39 mechanically-controlled. In contrast, the status of thermal comfort is difficult to be  
40 remained in the outdoor environments where wind speed and solar radiation change rapidly.  
41 Nevertheless, people continue contributing to build “comfortable” outdoor environments.  
42 In the 1990s, microclimates in urban areas gained notice [3]. Studies [2] have been carried  
43 out to assess the factors that could affect comfort in outdoor environments, such as  
44 streetscape aesthetics, noise, and air quality. Thermal and wind effects were found to be  
45 two of the most influential factors [2]. Thermal and wind conditions can be greatly

reformed by the arrangement of building clusters [4] and trees [5]. Thus, in the process of urban upgrades and city development, urban designers, architects and engineers will be continually challenged as the importance of outdoor thermal comfort increases. Thermal comfort is a complex concept and varies widely between objective and subjective evaluation [6]. Meteorological parameters strongly influence thermal sensation, which accounts for the objective part of thermal comfort [6]. It is widely known that six variables affect outdoor thermal sensation, including four meteorological variables (solar radiation, wind, ambient air temperature, and humidity) and two personal variables (activity level and clothing value) [3]. Liu et al. [7] observed long-term meteorological parameters and found air temperature was the most critical parameter in determining outdoor thermal sensation. However, outdoor conditions under building shadings were not their main concern. The shading conditions were considered by the study of Johansson [8], in which solar radiation were found to be vital factors affecting PET (Physiologically Equivalent Temperature). Attempts to quantify the effects of these six variables in defining outdoor thermal sensation and thermal comfort have been strongly pursued in recent years.

Many thermal indices addressing these six variables have been developed to evaluate and predict thermal sensation and thermal comfort, such as PET (Physiologically Equivalent Temperature) [9], SET\* (Standard Effective Temperature) [10], SPMV (Standard Predicted Mean Vote) [10], UTCI (the Universal Thermal Climate Index) [11] and the UCB model (a multi-node human body thermal regulation model developed by the University of California-Berkeley) [12] etc. Several research institutes have been using these thermal comfort indices when designing and assessing urban environments. Murakami et al. [13] combined the CFD simulation results with a radiation simulation of a Tokyo city block to produce a spatial distribution map of SET\* values. Middel et al. [5] increased the prediction accuracy of solar radiation spatial distribution by generating synthetic hemispherical fisheye views from Google Earth. A distribution map of PET based on the solar radiation prediction results was generated, hoping to increase the prediction accuracy of outdoor thermal comfort level [5]. Liu et al. [14] reported a simplified method combining with the measured thermal parameters and the simulated wind velocity by CFD to predict pedestrian level thermal comfort around an underneath-elevated building. Wind tunnel test results were also adopted in developing a thermal comfort map based on the PET index [15]. In general, there is a strong expectation of having a tool to accurately predict spatial outdoor thermal sensation and comfort when designing a sustainable community. But whether the existing thermal indices can accurately predict thermal sensation and comfort in an outdoor urban environment remains unknown and further assessment is needed.

These thermal indices were mainly developed by three approaches. The most direct and simple way is to build up a linear correlation between thermal sensation vote and a combination of meteorological parameters (solar radiation, wind speed, air temperature, and humidity) [16]. The models developed based on this approach are called the empirical models [7]. Liu et al. [7] correlated the thermal sensation vote with four outdoor meteorological parameters: air temperature, wind speed, absolute humidity and thermal radiation, and built up empirical models for Changsha based on long-term field observation. The empirical method is the most straightforward one to determine the relationship

between thermal sensation and meteorological parameters. However, it is region-specific. The linear correlation result can only be applied to a limited region and a group of subjects. Applying these results to model a region with a climate condition differs from that of the experimental location should be revised with correlation factors [17]. In the outdoors, the asymmetric distribution of solar radiation and transient wind environment form different microclimates, which makes the linear regression results more difficult to be applied.

The second approach is based on energy budget models, such as the PMV (Predicted Mean Vote) index [18]. The heat flux exchange between a human body and the ambient environment is the main concern of this approach. Existing thermal indices of this kind were all developed under steady thermal conditions, where subjects were assumed to reach a thermally equivalent status [18]. The thermal indices developed based on this assumption might not be suitable for the outdoors. Human bodies might be exposed to very different thermal conditions, such as simply walking from an air-conditioned indoor space (comfortably neutral condition) to an extreme outdoor environment (cold winter or hot summer). A thermally stable condition is practically impossible to be reached in this instance [18], which makes the existing thermal indices developed from energy balance models inappropriate for outdoor environments.

The third approach relates to thermo-physiological aspects [16, 18] such as SET\* [10], OUT-SET\* [19], PET [9], the UTCI [11], and the UCB model [12]. This approach focus on the stimulation of the thermal receptors located in the skin and the core, which perceive different levels of cold and warmth, then send signals to the brain [20, 21]. The main development of this approach in these years maintains at improving its details. The primitive ones were all based on the two-node model (the core node and the skin node), for instance, SET\* [10, 22, 23], OUT-SET\* [19] and PET [9]. Simply treating the human body as a two-node model often creates prediction errors when the thermal conditions are asymmetric and unstable. Xi et al. [22] discovered that the neutral SET\* varied when tested near different building blocks in the outdoors. Huang et al. [24] found different linear regression relations between PET and surveyed MTSV (Mean Thermal Sensation Vote) existed in different microclimates within one campus area. Human bodies are divided into more specific compartments in the UTCI compared to the early-stage thermal indices. In total, 12 compartments and 187 nodes are consisted in the UTCI model. It was expected to be available to solve the asymmetry problem by considering the heat transfer function separately for different body tissues and segments. Though this model has considered the rate of change of  $T_{skin}$  and  $T_{core}$  to cover transient conditions, its experimental validations was obtained at thermal uniform conditions [25]. Recently, some researchers attempted to verify its application in the outdoors: some focused on the operating parameters [26] and some on result comparisons [27]. From the results of Weihs et al. [26], asymmetric solar radiation condition could lead to misprediction in the UTCI model. When solar elevation was low, an error up to 2K appeared [26]. Acclimatization effects could also cause prediction difference in the outdoor usage of the UTCI model [28]. Longer exposure (minimum 30 minutes) could reduce prediction errors [28], which suggested that the UTCI model might perform better when thermal balance was established. Lai et al. [27] found substantial differences in the UTCI prediction results when comparing the climates in northern China and the Mediterranean [29]. UTCI is able to give better prediction results

than its older counterparts, but its application in the outdoors still needs further validation and amendment [30]. Whether it is the best choice for outdoor thermal condition prediction still remains controversy.

Similar physiological parameters were considered in the UCB model as in the UTCI model. However, the UCB model's prediction of thermal sensation and thermal comfort was more specifically based on skin temperature measurements on 19 local body parts and the core [12]. The experimental conditions of the UCB model were of a wider range than those of the UTCI model. Conditions including stable, transient, asymmetric, and uniform thermal environments were considered in the UCB model by controlling air temperatures within air sleeves focused on different body parts [12]. The UTCI model was developed based on heat transfer equations and empiric values from previous studies and a large amount of pre-existing human subject test data. In contrast, the UCB model was developed by building up a regression model between collected thermal sensation vote, thermal comfort vote, local skin temperature, core temperature and the rate of change of skin and core temperatures [12, 31, 32]. The experiment was conducted and validated in an indoor environment. The UCB model showed its strength in predicting thermal sensation in asymmetric and transient indoor environments. Zhou et al. [33, 34] compared the predicted mean skin temperature and thermal sensation results of the UTCI and UCB models against measured data of Chinese people in an indoor environment and found that the UCB model showed less discrepancy in the prediction of skin temperature. Zhou et al. [33] also formed transient and asymmetric environments by an air nozzle in constant air speed to validate the UCB prediction results, but the thermal environments formed by the air nozzle were much less complicated than the real outdoor environments. Other studies of the UCB model regarded its application. Han et al. [35] and Alahmer et al. [36] used it as a simulation tool to predict thermal comfort in vehicular spaces without conducting on-site measurements. Gao et al. [37] coupled the UCB model with a CFD simulation to evaluate occupants' thermal comfort in a displacement ventilation system and a mixing ventilation system with personalized ventilation.

Despite the potential advantages of the UCB model, yet, no existing studies have realized its application in the outdoor thermal sensation and comfort prediction. Moreover, this model has not been validated in an outdoor environment before, so whether the UCB model can give accurate prediction results in the fast-changing and asymmetric thermal environment of the outdoors remains unknown. The aims of the present study are to evaluate the potential application of the UCB model for rapidly changing and highly asymmetric outdoor environments and analyze the influence of meteorological parameters on thermal sensation from a new angle.

2. Methods

2.1. On-site survey

Our investigation was conducted on the campus of the Hong Kong Polytechnic University in southern China. Three sites were selected to cover different microthermal environments, as shown in Fig. 1. Sites 1 and 3, which were located in a passage of underneath-elevated buildings, represented semi-outdoor environments. The wind environment on Site 3 was more complex than Site 1 in the aspect of fast-changing wind speed. Site 2 was an open square that receive direct sunlight.

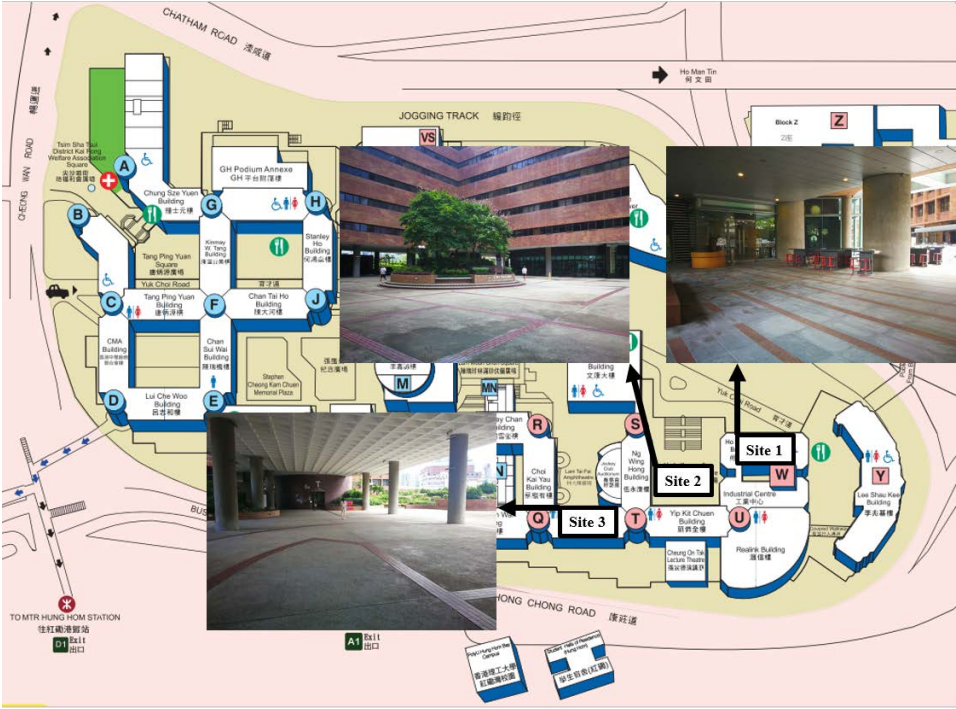


Fig.1 Survey locations

The field survey was conducted from March 30<sup>th</sup>, 2016, to December 12<sup>th</sup>, 2016. A total of 25 survey dates were involved, covering the typical climate features of cool winter, hot summer, and the transitional seasons in southern China. In total, 1107 questionnaire samples were collected. On each survey day, human subjects were invited to experience different microclimates following the sequence from Site 1 to Site 3. Subjects were asked to spend 15 minutes in each site, sitting, standing, or slowly walking around within a specific area, with their metabolic rates being recorded in the range between 0.79 and 2.34 Met. The mean value for the metabolic rate was 1.17 Met, with a standard deviation of 0.22 Met. The survey results that had a metabolic rate higher than 2.0 Met were abandoned in the data analysis. After a 15-minute adaptation to the given microthermal environment, each subject completed a thermal comfort questionnaire that was delivered to their mobile phone.

The thermal comfort questionnaire collected personal details (gender, age, height, weight, and clothing information), and asked questions about the subject's activity level, standing

direction, thermal sensation, thermal comfort, and wind and radiation preference. The ASHRAE seven-point thermal sensation scale [38] was adopted to evaluate the subjects' actual thermal sensation. The thermal comfort scale followed a five-point scale as very uncomfortable, uncomfortable, neutral, comfortable, and very comfortable. Table 1 describes the general information of human subjects. The clothing insulation is shown in Table 2. People's clothing insulation did not vary a lot when the season changed, this might owe to the warm winter in 2016 and the normal dressing habit of Hong Kong people.

Table 1. General Information of Human Subjects

	<i>Age</i>	<i>Weight (kg)</i> <i>Male/Female</i>	<i>Height (cm)</i> <i>Male/Female</i>	<i>Metabolic</i> <i>Rate (Met)</i>
<i>Mean</i>	25	67.33/52.17	172.9/161.2	1.17
<i>Median</i>	22	65/52	173/160	1.15
<i>Standard</i> <i>Deviation</i>	8.24	12.14/6.38	6.23/4.67	0.22
<i>Minimum</i>	15	43/40	161/148	0.79
<i>Maximum</i>	63	100/75	194/180	2.34

Table 2. Clothing Insulation

	<i>Clothing Value:</i> <i>T<sub>a</sub>&lt;30°C (Clo)</i>	<i>Clothing Value:</i> <i>T<sub>a</sub>≥30°C (Clo)</i>
<i>Mean</i>	0.48	0.48
<i>Median</i>	0.46	0.46
<i>Standard</i> <i>Deviation</i>	0.24	0.22
<i>Minimum</i>	0.16	0.16
<i>Maximum</i>	1.20	1.19

## 2.2. Measurement instructions and parameters

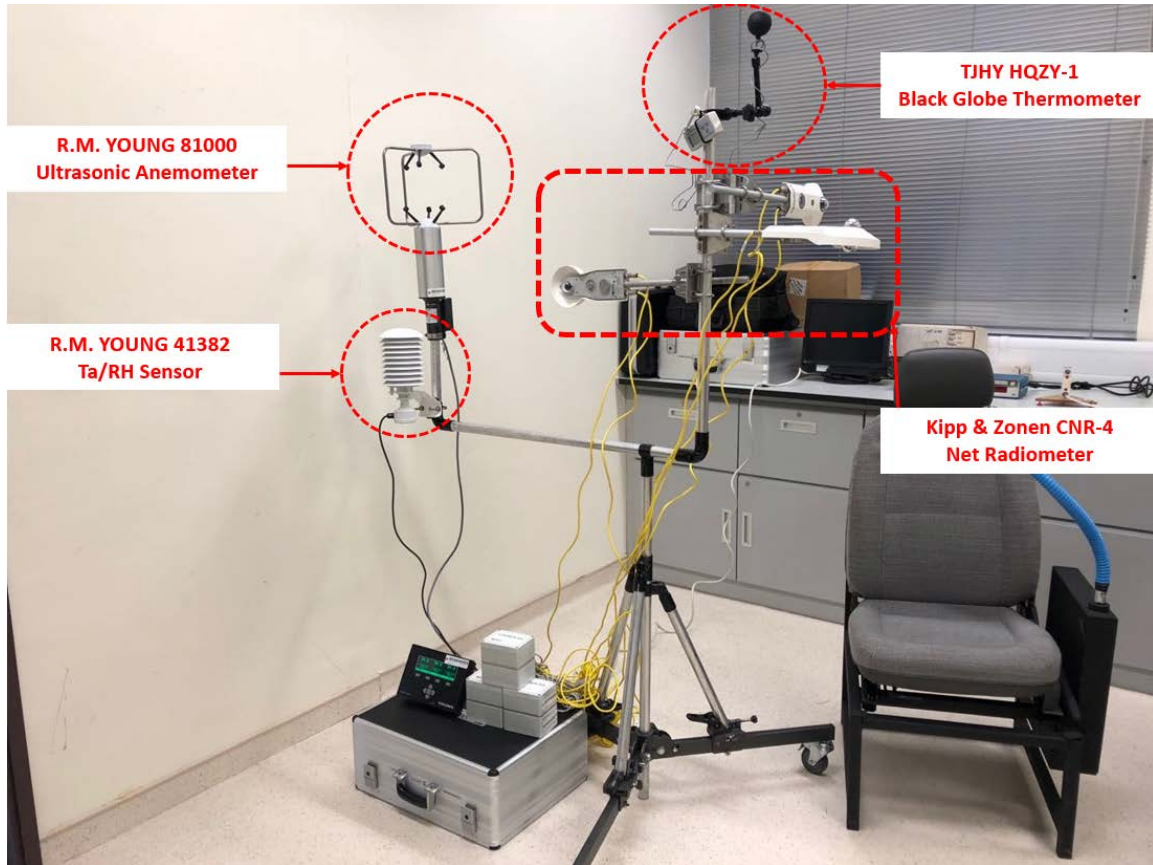


Fig. 2 Microclimate station

A microclimate station was constructed to collect the meteorological parameters at the survey location. As shown in Fig. 2, the devices were supported by a tripod at 1.5 m height. Real-time collection of eight parameters was performed in the microclimate station, including air temperature ( $T_a$ , °C), globe temperature ( $T_g$ , °C), relative humidity (RH, %), wind speed ( $v$ , m/s), wind direction, black globe temperature ( $T_b$ , °C), long-wave irradiance ( $L_i$ , W/m<sup>2</sup>), and short-wave irradiance ( $K_i$ , W/m<sup>2</sup>). A Ta/RH sensor (model 41382, R.M. YOUNG, USA) was used to collect air temperature and relative humidity data. An ultrasonic anemometer (model 81000, R.M. YOUNG, USA) recommended by ASHRAE handbook for meteorological parameters measurement [10], was able to measure both wind speed and direction. They were calculated from the difference in the times of flight of an ultrasonic pulse travel along two reverse directions on each axis. It should be noted that the monitored wind direction range is 0 to 360°, while the elevation range is limited to  $\pm 60^\circ$ . A black globe thermometer (model HQZY-1, TJHY, China) was used to measure the black globe temperature. In addition, a set of net radiometers (model CNR4, KIPP&ZONEN, the Netherlands) consisting of three pyranometer and pyrgeometer arms was used to collect long-wave and short-wave irradiation from six directions (the upper, ground and lateral directions). Both methods can be used to estimate the mean radiant temperature. The sampling interval for all parameters was set as 10 seconds. A more



specific information about the sensors used in the microclimate station has been reported in the authors' previous study [24].

## 2.3. Calculation method for radiant temperature

### 2.3.1. Mean radiant temperature

Mean radiant temperature is defined as “uniform temperature” in the ASHRAE fundamental handbook [10]. The calculation of mean radiant temperature was based on the six-directional technique, which was considered as the most accurate measurement method to obtain a  $T_{mrt}$  value in an outdoor environment, as stated in Eq. (2.1) [1].

$$T_{mrt} = \sqrt[4]{\sum_{i=1}^6 \frac{W_i(a_k K_i + \varepsilon_p L_i)}{\varepsilon_p \sigma}} - 273.1 \quad (2.1)$$

### 2.3.2. Radiant temperature from six enclosed surfaces

In the UCB model, it was assumed that a person was standing in an imaginary enclosed room (5 m × 5 m × 5 m) with different radiant temperatures of six wall surfaces. To simulate the asymmetric radiation condition in an outdoor environment, the long-wave and short-wave irradiation data collected in six directions by the radiometers was used in the calculation of six directional radiant temperatures,  $T_{mrt-i}$  ( $i = 1, 2, \dots, 6$ ). Then the equivalent temperatures of the six surfaces of the imaginary room were calculated. The radiometer was assumed to be at the center of the imaginary room, receiving equivalent radiation from the surface of the imaginary room. The surface of the radiometer facing in any one direction was assumed as a differential area, which formed an enclosure with those parts within the view in the imaginary room. Six surfaces formed six different enclosures. Within each enclosure, according to the method of calculating angle factor between a finite surface and a differential surface [39], six equations for calculating angle factors can be developed. The angle factor for the upper surface was 0.554126 in the imaginary enclosure and 0.111468 for the four lateral surfaces. Repeating this method in six directions, the equivalent surface temperature of the imaginary room can be obtained by solving the simultaneous linear equation of  $T_{mrt-i}^4$  ( $i = 1, 2, \dots, 6$ ) as shown in Eq. (2.2).

$$T_{mrt-i}^4 = T_{s1}^4 F_{i-s1} + T_{s2}^4 F_{i-s2} + T_{s3}^4 F_{i-s3} + T_{s4}^4 F_{i-s4} + T_{s5}^4 F_{i-s5} + T_{s6}^4 F_{i-s6} \quad (2.2)$$

## 2.3. Method of calculating $T_o$

The operative temperature  $T_o$  describes the total sensible heat exchange by convection and radiation between human and ambient environment [10]. As described in Eq. (2.3), the operative temperature can be defined as the weighted average of the mean radiant and ambient air temperature. In this equation, the radiative heat transfer coefficient can be calculated by Eq. (2.4), but it is not always possible to solve Eq. (2.4) due to a lack of information for  $T_{cl}$ . Fortunately,  $h_r$  is nearly constant for most conditions, and a value of 4.71 W/m<sup>2</sup>K is sufficient for most calculations [38]. However, the equations for estimation of  $h_c$  are determined by relative wind speed. The highest wind speed for a standing person

listed in the ASHRAE standard 55 table [38] was 1.5 m/s, which was not applicable for some of our experimental conditions. Thus, de Dear's equation [40] was referred in this study, in which the experimental wind speed for  $h_c$  regression was up to 5 m/s. The estimation of  $h_c$  is shown in Eq. (2.5).

$$T_o = \frac{h_r T_{mrt} + h_c T_a}{h_r + h_c} \quad (2.3)$$

$$h_r = 4\varepsilon_p \sigma \frac{A_r}{A_D} \left( 459.7 + \frac{T_{cl} + T_{mrt}}{2} \right)^3 \quad (2.4)$$

$$h_c = 10.3v^{0.6} \quad (2.5)$$

#### 2.4. A brief description of the UCB model

The UCB model was developed from thermo-physiological measurements (skin and core temperatures) and was then validated with real passengers sitting in automobiles within a climate chamber [12]. It was hypothesized in this model that the thermal sensation feeling was based on a self-thermoregulation system, which was triggered by the sensory organs (thermal receptors) located in the skin, spin and some abdominal organs [41]. The number and depth of warm and cold receptors varied from part to part in human body [41], which was the reason a multi-node model should be adopted when the un-uniform thermal environment was concerned. During the experiment, human subjects were asked to wear air sleeves of conditioned air that enclosed specific body segment to force the individual body parts through a range of temperatures. The subjects' local skin temperatures and core temperatures were measured and they were repeatedly surveyed for local and whole-body sensation and comfort level [42]. An extended ASHRAE seven-point scale, adding "+4 very hot" and "-4 very cold", was used to evaluate thermal sensation [12]. The thermal comfort level scale was a symmetric six-point scale : "+4 very comfortable", "+2 comfortable", "0 just comfortable", "-0 just uncomfortable", "-2 uncomfortable", "-4 very uncomfortable" [32]. To obtain thermal responses in individual body segments under transient and asymmetric conditions, most of the tests involved cooling local body parts under warm conditions followed by warm recovery, and a limited number of tests warmed local body parts under cool conditions [12].

In the UCB model, the local thermal sensation was divided into two parts: static and dynamic parts (Eq. (2.6)) [12]. The static local sensation was a logistic function of the difference between local skin temperature and its set point, while the dynamic local sensation was determined by the derivatives of skin and core temperature [12]. The entire local sensation equation followed the form as Eq. (2.7) [12]. The weight of each local body part in determining overall thermal sensation was obtained from experimental data. The overall thermal sensation was considered by two different conditions separately: "no opposite sensation" and "opposite sensation" conditions [31]. If no body parts feel significantly opposite to the other body parts, it was termed the "no opposite sensation" condition; otherwise, "opposite sensation" condition was termed [31]. Each body part accounted for a certain weight in determining overall thermal sensation if "no opposite sensation" condition was considered [31]. If "opposite sensation" condition was considered,

the whole body sensation led the overall thermal sensation while the “opposite parts” modified it [31].

$$\text{Local Sensation} = \text{Sensation}_{\text{static}} + \text{Sensation}_{\text{dynamic}} \quad (2.6)$$

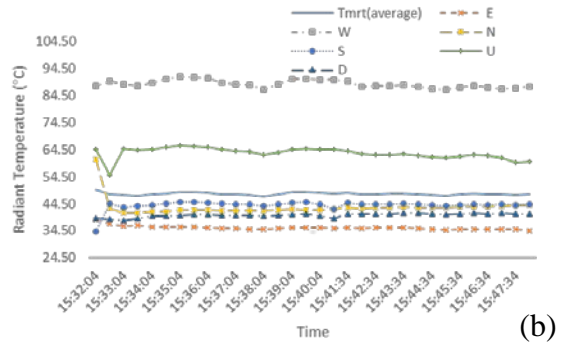
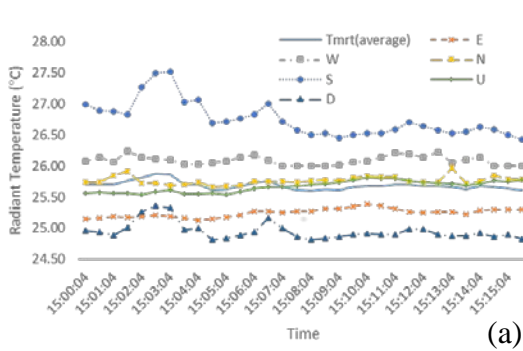
$$\text{Local Sensation} = \int (T_{\text{skin},i}, \frac{dT_{\text{skin},i}}{dt}, \bar{T}_{\text{skin}}, \frac{dT_{\text{core}}}{dt}) \quad (2.7)$$

In the UCB model software, the collected personal details can be input in the body builder, such as height, weight, age, and gender. A clothing modeler was embedded in the UCB model, normal summer and winter clothing can be found in the clothing library. For each specific human subject, clothing as recorded in the survey was selected in the UCB simulation.

The air temperature and air speed can be set inside the imaginary room. The air temperature was set as uniform during the simulation, and the air speed had a maximum of 2 m/s. The asymmetric solar radiation condition was set using the “panel condition setting” in the software. To better simulate solar conditions, each panel in the imaginary room was set as a large window of 4.99 m width and height, with a 0.01 m wide wall frame. Each panel was set to the calculated surface radiant temperature according to its direction. The imaginary subject was located at the center of the room, in the actual standing direction as they were during the on-site experiment. The absorption coefficient and emissivity were both set as 1.0 for the open window in the imaginary room to ensure the real radiant temperature as on-site.

### 3. Results and discussion

#### 3.1. Meteorological data analysis



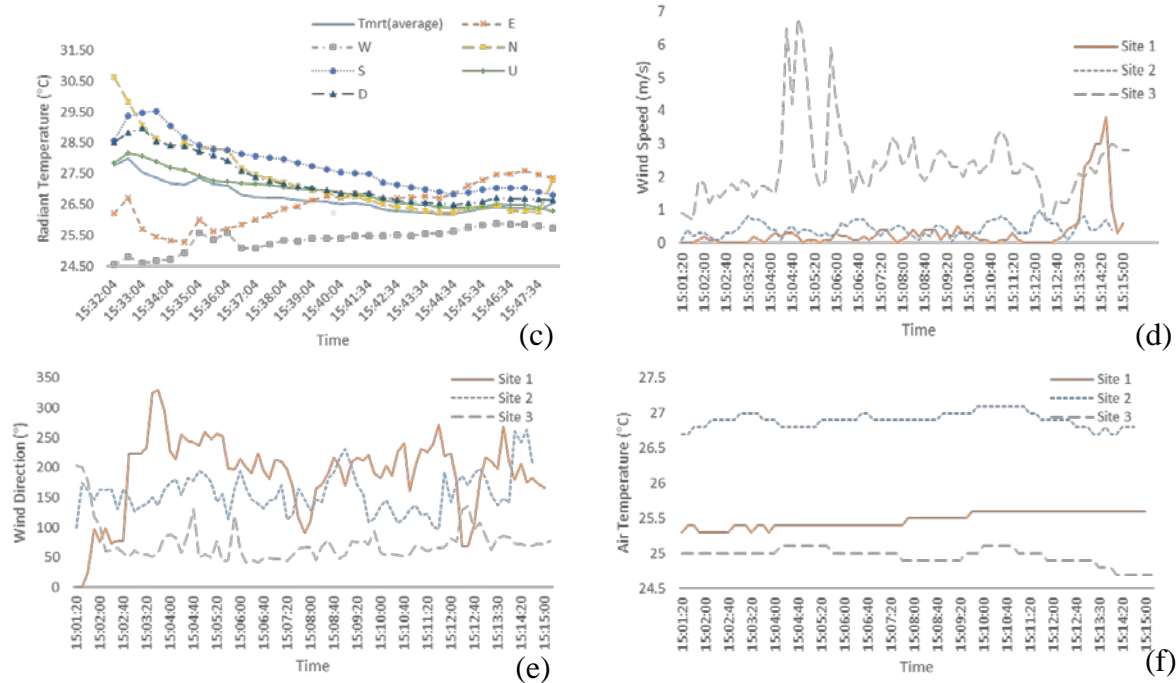
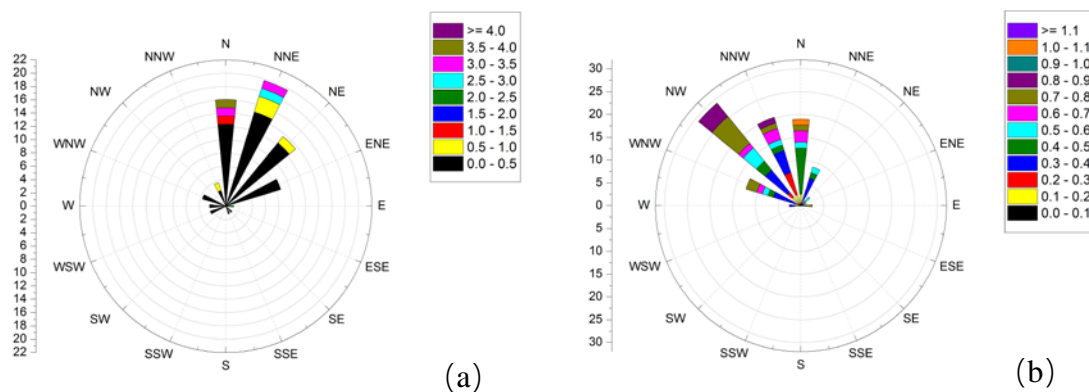


Fig. 3 The meteorological data measurement results obtained by the microclimate station: (a) radiant temperature measured at Site 1; (b) radiant temperature measured at Site 2; (c) radiant temperature measured at Site 3; (d) wind speed measurement results for the three sites; (e) wind direction measurement results for the three sites; (f) air temperature measurement results for the three sites



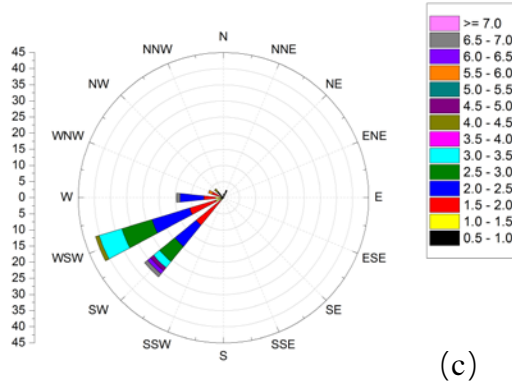


Fig. 4 The wind rose distribution (a) Wind rose distribution at Site 1 (b) Wind rose distribution at Site 2 (c) Wind rose distribution at Site 3

Fig. 3 shows the meteorological data collected by the microclimate station in one typical survey day. The distribution of the solar radiation values from three survey sites are shown in Fig. 3 (a) to (c). A large variation of solar radiation was visible from six directions. These data were collected from 3:00 PM to 4:00 PM, for 15 minutes at each survey site. Although Sites 1 and 3 were sheltered by the underneath-elevated building block, the difference between these two sites was noteworthy. The solar radiation condition was greatly affected by the surrounding building clusters and sampling sites. There was a large directional difference in the radiation temperatures. The radiation temperature from the south was higher than that from the other directions at Site 1. It was followed by the radiation coming from the west. At Site 3, radiation from the south was slightly higher than the other directions, and radiation from the west was the lowest. Low radiation temperatures from the ground was detected at Sites 1 and 3; while, at Site 2, which received direct solar radiation, the radiation temperature from the ground was similar to that from the other directions. In the Site 2 dataset, the radiation temperatures from the upper side and the west were much higher than from other directions. Shadings can effectively reduce radiation coming from all directions, especially from the above.

Fig. 3 (d to f) shows the instantaneous distribution of wind speed, wind direction, and air temperature respectively. The air temperature at the three sites was fairly stable during the sampling time; the change remained within 0.5 °C. The unstable parameters came from windy environments, especially those in the urban area and surrounded by tall buildings. The highest wind speed was detected at Site 3. The transient wind speed could reach 7 m/s and generally stayed at around 2 to 3 m/s. The lowest wind speed was recorded at Site 2, which was around 0.4 m/s. Wind environment can differ greatly from location to location, even within one campus, affected by building arrangement and structure. The wind direction changed frequently during the survey period, but most of the time it stayed at the main direction as shown in the wind rose figure (Fig. 4). In the recording day, the wind mainly came from the NNE for Site 1, from the NW for Site 2, and from the WSW for Site 3. For Sites 1 and 3, the wind could pass through the underneath of the elevated building block without much obstruction. Thus, the wind followed the seasonal wind direction and fluctuated at a relatively stable range. Three buildings surrounded the measurement point at Site 2, so the wind flowed through Site 2 at pedestrian height was blocked. The wind

direction at Site 2, therefore, was more dispersed. Wind environments from the outdoor settings were much more complex than that indoors, introducing further uncertainty when defining thermal sensation and thermal comfort. For indoor thermal comfort studies, it is recommended that omnidirectional anemometers should be used for air velocity measurement to ensure the accuracy [10, 43]. Limited by the measurement range of elevation angle in the ultrasonic anemometer of the microclimate station, measurement of omnidirectional air velocity might not be accurate where downdraft velocity was significant. An omnidirectional ultrasonic anemometer should be considered for further outdoor thermal comfort experiment.

### 3.2. Comparison of the surveyed TSV and simulated TSV (by the UCB model) over the whole range of operative temperature

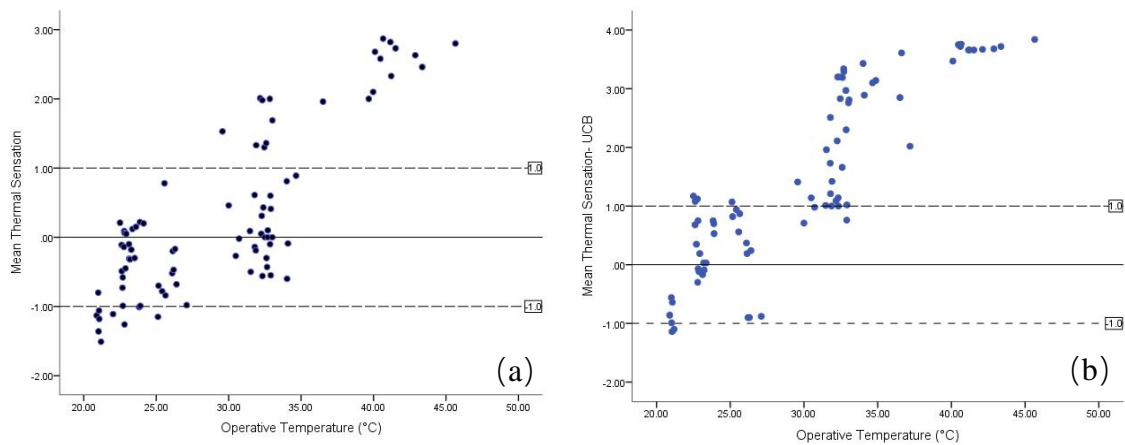


Fig. 5 Thermal sensation data over the experiment period (a)  $T_{op}$  vs TSV; (b)  $T_{op}$  vs TSV-UCB

Fig. 5 presents the distribution of mean thermal sensation which covers all the experiment dates. Fig. 5 (a) covers subjects' actual thermal sensations from cool winter to hot spring in Hong Kong, which is a typical representation of hot and humid Asian climate. The collected air temperatures ranged from 21°C to 36 °C. In 2016, Hong Kong had a warm winter, so thermal sensation in cold winter conditions was not able to be collected. However, the transitional seasons and the summer period during the experiment represent the city's typical climate. Fig. 5 (b) shows the UCB simulated TSV results.

When people expressed their thermal sensation in the range of acceptable conditions (between “-1 TSV” and “+1 TSV”), the mean operative temperature was 27 °C. The corresponding operative temperature was 26°C when the simulated TSV remained at an acceptable range, which was close to the on-site survey result. Observed from Fig. 5 (a), the operative temperature which remained at acceptable condition was in the range of 20 °C to 35 °C. By contrast, most of the accepted TSV concentrated at around 25 °C in the simulated TSV result. The range of acceptable operative temperature in the outdoors was much higher than that recorded indoors (in the literature, the range of acceptable temperature in an indoor environment was between 18 °C and 26.8 °C [44]). The simulated

TSV clustered at “+1 TSV” to “+3.2 TSV” when the operative temperature was in the range of 30 to 35 °C (Fig. 5 (b)), which was much higher than the voted TSV. This phenomenon indicates that people had a higher tolerance for high temperatures when exposed to the outdoor environment.

It is interesting that there is a large variance shown in the range of voted thermal sensation around the operative temperature between 30 °C and 35 °C, from “-0.7 TSV” to “+2 TSV”. The long TSV span denotes that some factors in the outdoor environments could contribute more in decreasing subjects’ thermal sensation in the recorded cases. The authors’ previous study based on the climate characteristics of Hong Kong has pointed out solar radiation and wind speed were two main factors that create thermal sensation difference of short-term exposure by comparing three microclimate conditions where air temperature and humidity remained similar [24]. Thus, wind and solar radiation will be the focus of the following analysis.

In the range of 40 °C to 45 °C, where high solar radiation contributed to a further increase of operative temperature, the voted thermal sensation did not present an obvious increasing trend. The seven-point scale in ASHRAE standard 55 [38] might not be appropriate for people to express their thermal sensation in hot summer outside, especially when high radiation circumstances are encountered. Instead, the nine-point scale used in the UCB model [12], adding “+4 TSV” and “-4 TSV” to express “too hot” and “too cold” respectively, is recommended for application in the outdoor thermal comfort experiment and our further experiment.

### 3.3. Comparison of the surveyed TSV and simulated TSV (by UCB model) over the change in wind speed

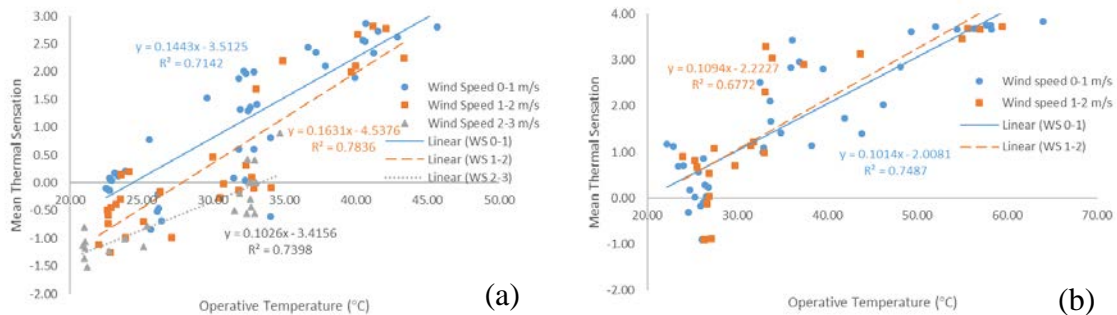


Fig. 6 Comparison of on-site TSV and UCB-simulated TSV over a range of wind speeds (a) on-site data, (b) UCB data

To analyze the effects of wind speed in decreasing thermal sensation in outdoor environments, the collected data was split into three groups according to the level of wind speed in one experimental period. The group with a wind speed lower than 1 m/s was termed the breeze group; between 1 m/s and 2 m/s was termed the mild wind group; and between 2 m/s and 3 m/s was termed the strong wind group. Generally, the strong wind



group was only detected at Sites 1 and 3, where wind could blow through the elevated level. But the operative temperature of Sites 1 and 3 was not as high as Site 2 due to the shading created by the elevated level. Thus, no data could be collected for the strong wind group when the operative temperature was high.

Linear regression was performed to describe the trend of thermal sensation with the increase of operative temperature. The R square for each linear regression was higher than 0.7. From Fig. 6 (a), it is obvious that when compared to the breeze group, the mild wind made people feel cooler when the operative temperature remained the same. The cooling effect was stronger when the operative temperature was lower than 34 °C. When the operative temperature was higher than 34 °C, the cooling effect brought on by increased wind speed was weakened. This was the interval where the radiant temperature was high. A *t*-test was conducted to verify the cooling effect of increased wind speed within this interval. The *p*-value for the breeze group and the mild wind group was 0.098 (larger than 0.05), demonstrating that increasing the wind speed to mild wind group did not create a thermal sensation difference when the operative temperature was higher than 34 °C. ANOVA analysis (An analysis of variance) was conducted to test the differentiation of voted thermal sensation between the three wind speed groups. Only the data lower than 34 °C was used in the analysis. They all satisfied the homogeneity test of variance, and thus the ANOVA result analyzed with the least significant difference (LSD) method was confidential. The *p*-value for the breeze and mild wind groups was 0.005 (lower than 0.05), indicating that increasing wind speed from 0-1 m/s to 1-2 m/s can create a significant thermal sensation difference. Similar results were found when the breeze and strong wind groups were compared. However, the *p*-value for the mild wind and strong wind groups was 0.092 (larger than 0.05), meaning that further increasing the wind speed from 1-2 m/s to 2-3 m/s did not make people feel cooler.

Considered the simulated thermal sensation results, only the breeze group and mild wind group were simulated. Because the UCB model was developed in an indoor environment, where wind speed above 2 m/s rarely occurs, simulations of wind speed higher than 2 m/s were not able to be performed in the development stage of the UCB model software. The simulated thermal sensation result (Fig. 6 (b)) did not show any difference between two different wind speed groups. The dataset from the breeze group highly coincided with that of the mild wind group in full range of the operative temperatures. The *t*-test results supported this finding, with a *p*-value of 0.319 (much larger than 0.05). Increasing the wind speed from 0-1 m/s to 1-2 m/s did not create a difference in the predicted thermal sensation. It seems the cooling effect of increasing wind speed in an outdoor environment were more obvious than in the experimental results indoors. People were more sensitive to changes in wind speed when outdoors.

The most crucial part of the UCB model was building the prediction function of subjects' thermal sensation. The thermal sensation prediction model was developed from the dataset obtained from the local skin temperature control experiment, which was performed by controlling the air temperature within air sleeves [12]. The heat was transferred to the air sleeves mostly through conduction. The cooling effect of air movement was weakened in the UCB model. Moreover, the highest tolerable wind speed was 0.8 m/s in an indoor



environment, as recommended by ASHRAE 55 [38]. Wind speeds higher than this range lead to draft discomfort indoors. There is no doubt that the cooling effect of higher wind speeds was not the focus of the UCB model, as it was intended to predict thermal conditions indoors and in vehicles. Further experiments that combine the UCB model structure with the meteorological parameters and the physiological features of subjects in outdoor environments should focus more on the amendment of heat conduction and convection terms. The reasons that further increasing wind speed from 1-2 m/s to 2-3 m/s did not create thermal sensation difference should also be explained using physiological and psychological data.

### 3.4. Comparison of the surveyed TSV and simulated TSV (by the UCB model) over the change of solar radiation levels

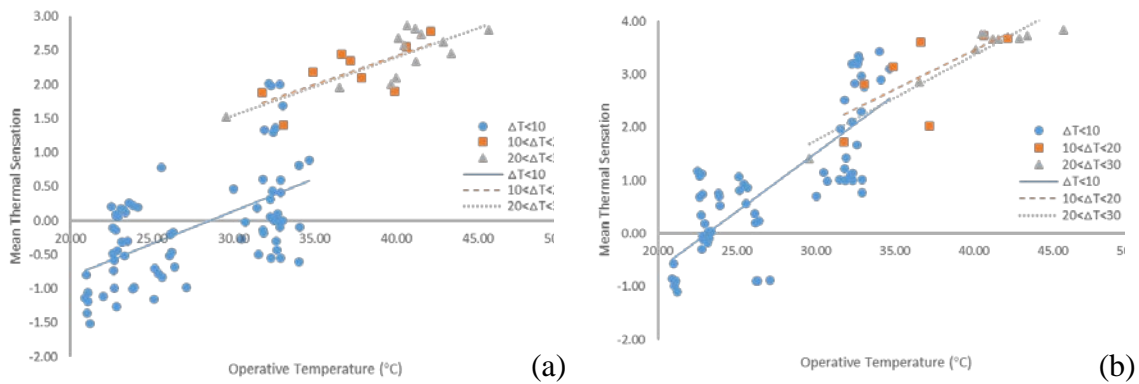


Fig. 7 Comparison of on-site TSV and UCB-simulated TSV at different solar radiation levels (a) on-site data, (b) UCB data

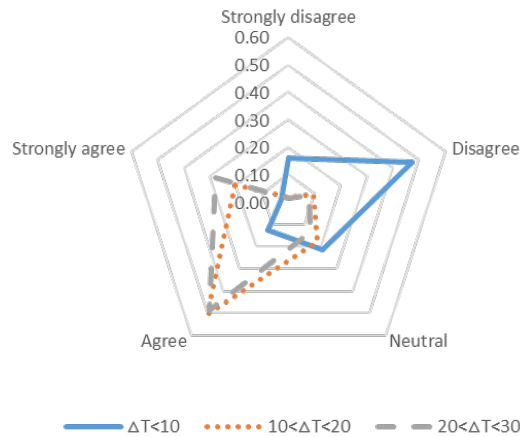


Fig. 8 Percentage distribution of people's feelings on sun radiation

Fig. 7 shows the comparison of thermal sensation result difference (on-site surveyed data and UCB-simulated data) for different solar radiation levels. Solar radiation was divided into three groups according to the difference between mean radiant temperature and air temperature ( $\Delta T$ ). When  $\Delta T$  was lower than 10 °C, it was termed the low radiation group;

when  $\Delta T$  was between 10 °C and 20 °C, it was termed the mid radiation group; and when  $\Delta T$  was between 20 °C and 30 °C, it was termed the high radiation group. The low radiation group only appeared in the operative temperature range of 20 °C to 35 °C, whereas the mid and high radiation groups appeared in the operative temperature range of 29 °C to 45 °C. The limitation of the distribution of different solar radiation levels was mostly attributed to the climate characteristics of Hong Kong.

From the on-site data (Fig. 7 (a)), it is obvious that the surveyed thermal sensation in the low radiation group is much lower than that in the mid and high radiation groups. It is interesting to note that although the operative temperature was as high as 30 °C to 35 °C, subjects still noted their thermal feelings to be acceptable (slightly warm) as long as the radiation level was low. However, this range of operative temperature was noted as unacceptable in indoor environments when the relative humidity was higher than 60% [38] (in a typical summer of Hong Kong, the relative humidity is normally higher than 60%). This phenomenon indicates that people could better tolerate high air temperatures outdoors in the case of the radiation level was acceptable. In Fig. 7 (a), the trend line of the low radiation group is not in the same line as the mid and high radiation groups, but the slopes are similar. The sudden change of TSV demonstrates that even medium radiation could lead to intolerable hot feelings outdoors. Upgrading solar radiation from low- to mid-level could significantly increase people's thermal sensation levels. To understand subjects' feelings in radiation, the question "Do you agree that the sun is annoying?" was asked in the questionnaire. Five answers were provided: "strongly agree", "agree," "neutral", "disagree", and "strongly disagree". Fig. 8 shows the percentage of answers for each category. Nearly 50% of the subjects voted that the sun was not annoying when radiation was low. However, unpleasant feelings regarding sun radiation were strongly expressed when the radiation was medium or high.

Both the sudden increase of thermal sensation votes shown in Fig. 7 (a) and the change of subjects' opinions shown in Fig. 8 with increasing radiation levels illustrate that subjects were highly sensitive to the changes in the solar radiation level. People preferred a low radiation level and disliked even medium-level radiation. However, the trend lines of the low and mid radiation groups in the UCB-simulated thermal sensation results almost coincided. The leap in thermal sensation level when solar radiation changed from low to medium did not happen in the simulated result. The UCB model tended to give higher TSV results than the field-surveyed data in the low radiation group. Although the UCB model used an extended nine-point thermal sensation scale to ensure accurate expression of thermal sensation in extreme hot and cold environments, thermal sensation in a mild thermal environment should not be affected. However, the TSV from the UCB model was concentrated at the warm side, whereas the field-surveyed data was clustered on the cool side, in the operative temperature range of 20 °C to 25 °C. In the range of 30 °C to 35 °C of the low-radiation group, the UCB-simulated TSV was concentrated at "+1 slightly warm" and "+3 hot", whereas the field-surveyed TSV corresponding to those temperatures ranged from "-1 slightly cool" to "+1 slightly warm". The phenomenon observed in the survey was not reflected in the simulation data. According to the UCB model validation and the indoor survey results from Zhou et al. [33], the discrepancy was only about 0.5 TSV scale

unit. The UCB model seems to have larger discrepancy when predicting outdoor thermal sensation than indoor thermal sensation, especially under low-radiation conditions.

It is difficult to compare the UCB-simulated result and the on-site surveyed result when the operative temperature is high, owing to the application of different thermal sensation scales. However, both the surveyed points and the simulated points show that the TSV data for medium and high radiation coincide. There is no leap between the mid and high radiation groups.

### 3.5. Thermal sensation sensitivity to wind speed and mean radiation temperature

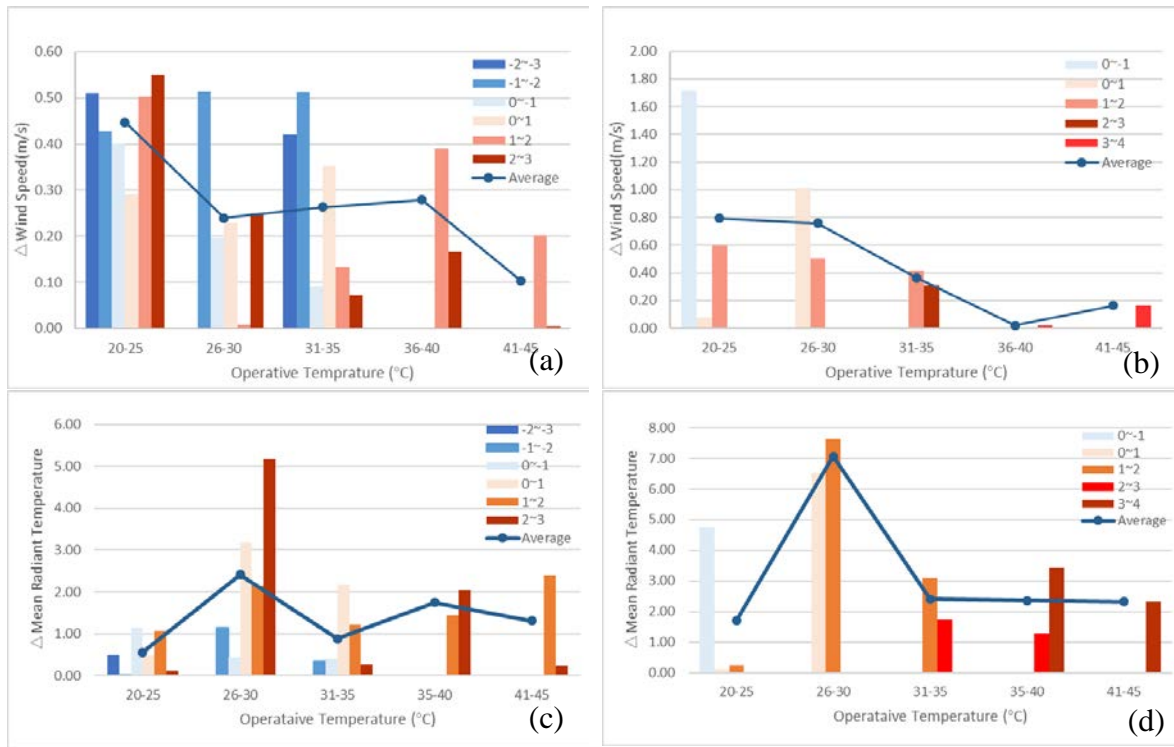


Fig. 9 Thermal sensation sensitivity to wind speed (a: on-site data, b: UCB-simulated data) and mean radiation temperature (c: on-site data, d: UCB-simulated data)

This part of the study aims to discover thermal sensation sensitivity to wind and mean radiant temperature in different ranges of operative temperature. The whole dataset was separated into five groups of operative temperature, which spanned 5 °C each. Within each operative temperature group, the data were organized according to the level of thermal sensation. By changing each thermal sensation level, the change in mean radiant temperature or wind speed can be obtained. If the change in the observed parameter was large when the thermal sensation level changed one degree, the subjects were not sensitive to the observed parameter in the given range. On the contrary, if a slight change in the observed parameter can lead to a one-degree change in thermal sensation, the subjects were highly sensitive to the observed parameter.

When Fig. 9 (a) and (b) are compared, it is noticeable that the average change of wind speed causing a one-degree change of thermal sensation was much smaller than that of the UCB simulated result in each operative temperature range. As the UCB model was developed based on the experimental data obtained in the indoor chamber, the comparison result illustrates that subjects in the outdoor environment were more sensitive to the change of wind speed in the outdoors compared to the indoors. However, both two figures (Fig. 9 (a, b)) show much smaller scale in the change of wind speed when the operative temperature was higher than 40 °C. Thus, subjects became more sensitive to wind environment when the extreme hot condition happened in an outdoor environment. This finding is an explicit illustration that the city planners in the tropical and subtropical area should pay more attention to the wind environment in the neighborhood during the design stage. The building structures that improve air movement around building blocks, e.g. the elevated building block design in the campus of Hong Kong Polytechnic University, should be advocated.

Both the on-site data (Fig. 9 (c)) and the simulated data (Fig. 9 (d)) show that when the operative temperature was in the range of 26 °C to 30 °C, which was around the neutral state operative temperature (27 °C) in the outdoor environment, the subjects were less sensitive to solar radiation. The allowable change in mean radiant temperature in this range was much higher than that in any other operative temperature ranges. As shown in the on-site data (Fig. 9 (c)), a mean radiation temperature change of less than 2 °C can lead to a one-degree change in thermal sensation, except in the range 26 °C to 30 °C. This value was smaller than that of the simulated result. Hence, people in outdoor environments might be more sensitive to the changes in solar radiation than predicted in the UCB model.

The sensitivity comparison of the UCB-simulated result and the on-site surveyed result further illustrates that people were more sensitive to changes in wind speed and solar radiation in outdoor environments than in indoor environments. The sensitivity to meteorological parameters varied under different operative temperature ranges. It cannot be generalized to one specific number. A reasonable inference is that the sensitivity of different body parts to these parameters might be changed with the range of operative temperature. The dominating body parts when defining overall thermal sensation might be varied as well. Therefore, based on the outline of the UCB model, for higher accuracy in predicting outdoor thermal comfort, further experiments in detecting skin and core temperatures and relating these physiological parameters to outdoor thermal sensations should be performed.

#### 4. Conclusions

This study compared the surveyed thermal sensation data and the simulated data using the UCB model and verified its usage in outdoor environments from a sensitivity point of view. Two fast-changing meteorological parameters – wind speed and solar radiation – were discussed in this study.

The UCB model did not respond well to the changes in wind speed. The on-site data show that increasing wind speed from breeze group to mild wind group could create a

considerable cooling effect when the operative temperature was lower than 34°C. However, the UCB-simulated results showed no thermal sensation difference between two wind speed groups. Subjects' thermal sensation in an actual outdoor environment was more sensitive to wind environment than predicted in the model.

Subjects better tolerated high air temperatures outdoors when the solar radiation was low. They preferred low radiation and disliked medium or high radiation. The mid and high radiation groups made a leap in TSV compared with the low radiation group in the on-site data, but this was not observed in the UCB-simulated data. The UCB model may over-predicted the TSV of the low radiation group. The sensitivity of these two parameters was examined under different operative temperature ranges. Subjects' sensitivity to wind speed and solar radiation did not remain the same at all operative temperature ranges. They were more sensitive to changes in wind speed when the environment got hotter.

Their sensitivity to mean radiant temperature remained more or less the same, except for the condition that subjects stayed in neutral thermal status. The UCB-simulated data showed a similar pattern. However, for a one-degree change in TSV, the UCB data allowed less change in wind speed and solar radiation than the on-site data, which implies that the UCB model was less sensitive to these two parameters than the actual outdoor survey results showed.

To better reveal the relation between outdoor transient and asymmetric thermal environment and thermal sensation feelings and for the purpose of better application of the multi-nodal thermal regulation model in the outdoors, additional direct measurement of subject physiological parameters such as core and skin temperatures in outdoor environments may be helpful.

## **Acknowledgements**

The work described in this paper was fully supported by a grant from the Research Grants Council of the Hong Kong Special Administrative Region, China (Project No. C5002-14G). The authors wish to thank Dr. Zhang Hui at CBE, UC-Berkeley for her help in running the multi-nodal regulation model.

- [1] N. Kántor, A. Kovács, T.-P. Lin, Looking for simple correction functions between the mean radiant temperature from the “standard black globe” and the “six-directional” techniques in Taiwan, *Theoretical and applied climatology* 121(1-2) (2015) 99-111.
- [2] M.J. Soligo, P.A. Irwin, C.J. Williams, G.D. Schuyler, A comprehensive assessment of pedestrian comfort including thermal effects, *Journal of Wind Engineering and Industrial Aerodynamics* 77 (1998) 753-766.
- [3] E. Arens, P. Bosselmann, Wind, sun and temperature—Predicting the thermal comfort of people in outdoor spaces, *Building and Environment* 24(4) (1989) 315-320.
- [4] J. Niu, J. Liu, T.-C. Lee, Z. Lin, C.M. Mak, K.-T. Tse, B.-S. Tang, K.C.S. Kwok, A new method to assess spatial variations of outdoor thermal comfort: Onsite monitoring results and implications for precinct planning, *Building and Environment* 91 (2015) 263-270.
- [5] A. Middel, J. Lukasczyk, R. Maciejewski, Sky View Factors from Synthetic Fisheye Photos for Thermal Comfort Routing—A Case Study in Phoenix, Arizona, *Urban Planning* 2(1) (2017) 19-30.
- [6] M. Nikolopoulou, K. Steemers, Thermal comfort and psychological adaptation as a guide for designing urban spaces, *Energy and Buildings* 35(1) (2003) 95-101.
- [7] W. Liu, Y. Zhang, Q. Deng, The effects of urban microclimate on outdoor thermal sensation and neutral temperature in hot-summer and cold-winter climate, *Energy and Buildings* 128 (2016) 190-197.
- [8] E. Johansson, Influence of urban geometry on outdoor thermal comfort in a hot dry climate: a study in Fez, Morocco, *Building and environment* 41(10) (2006) 1326-1338.
- [9] P. Höppe, The physiological equivalent temperature—a universal index for the biometeorological assessment of the thermal environment, *International journal of Biometeorology* 43(2) (1999) 71-75.
- [10] A.S. Committee, ASHRAE handbook: fundamentals 2017, American Society of Heating, Refrigerating and Air-Conditioning Engineers 2017.
- [11] D. Fiala, G. Havenith, P. Bröde, B. Kampmann, G. Jendritzky, UTCI-Fiala multi-node model of human heat transfer and temperature regulation, *International journal of biometeorology* 56(3) (2012) 429-441.
- [12] H. Zhang, E. Arens, C. Huizenga, T. Han, Thermal sensation and comfort models for non-uniform and transient environments: Part I: Local sensation of individual body parts, *Building and Environment* 45(2) (2010) 380-388.
- [13] S. Murakami, R. Ooka, A. Mochida, S. Yoshida, S. Kim, CFD analysis of wind climate from human scale to urban scale, *Journal of Wind Engineering and Industrial Aerodynamics* 81(1) (1999) 57-81.
- [14] J. Liu, J. Niu, Q. Xia, Combining measured thermal parameters and simulated wind velocity to predict outdoor thermal comfort, *Building and Environment* 105 (2016) 185-197.
- [15] Y. Du, C.M. Mak, T. Huang, J. Niu, Towards an integrated method to assess effects of lift-up design on outdoor thermal comfort in Hong Kong, *Building and Environment* 125 (2017) 261-272.
- [16] D. Lai, X. Zhou, Q. Chen, Modelling dynamic thermal sensation of human subjects in outdoor environments, *Energy and Buildings* 149 (2017) 16-25.
- [17] T.P. Lin, A. Matzarakis, Tourism climate and thermal comfort in Sun Moon Lake, Taiwan, *International Journal of Biometeorology* 52(4) (2008) 281-290.
- [18] P. Höppe, Different aspects of assessing indoor and outdoor thermal comfort, *Energy and buildings* 34(6) (2002) 661-665.
- [19] J. Pickup, R. de Dear, An outdoor thermal comfort index (OUT\_SET\*)-part I-the model and its assumptions, *Biometeorology and urban climatology at the turn of the millenium. Selected papers from the Conference ICB-ICUC, 2000*, pp. 279-283.
- [20] A. Craig, Pain mechanisms: labeled lines versus convergence in central processing, *Annual review of neuroscience* 26(1) (2003) 1-30.

- [21] J.E. Hall, Guyton and Hall textbook of medical physiology, Philadelphia: Saunders Elsevier (2011).
- [22] T. Xi, Q. Li, A. Mochida, Q. Meng, Study on the outdoor thermal environment and thermal comfort around campus clusters in subtropical urban areas, *Building and Environment* 52 (2012) 162-170.
- [23] A. Gagge, Standard effective temperature-A single temperature index of temperature sensation and thermal discomfort, Proc. of the CIB Commission W45 (Human Requirements), Symposium, Thermal Comfort and Moderate Heat Stress, 1973, Building Research Station, 1973, pp. 229-250.
- [24] T. Huang, J. Li, Y. Xie, J. Niu, C.M. Mak, Simultaneous environmental parameter monitoring and human subject survey regarding outdoor thermal comfort and its modelling, *Building and Environment* 125 (2017) 502-514.
- [25] D. Fiala, K.J. Lomas, M. Stohrer, Computer prediction of human thermoregulatory and temperature responses to a wide range of environmental conditions, *International Journal of Biometeorology* 45(3) (2001) 143-159.
- [26] P. Weihs, H. Staiger, B. Tinz, E. Batchvarova, H. Rieder, L. Vuilleumier, M. Maturilli, G. Jendritzky, The uncertainty of UTCI due to uncertainties in the determination of radiation fluxes derived from measured and observed meteorological data, *Int J Biometeorol* 56(3) (2012) 537-55.
- [27] D. Lai, D. Guo, Y. Hou, C. Lin, Q. Chen, Studies of outdoor thermal comfort in northern China, *Building and Environment* 77 (2014) 110-118.
- [28] E.L. Krüger, C.A. Tamura, P. Bröde, M. Schweiker, A. Wagner, Short-and long-term acclimatization in outdoor spaces: Exposure time, seasonal and heatwave adaptation effects, *Building and Environment* 116 (2017) 17-29.
- [29] F. Salata, I. Golasi, R. de Lieto Vollaro, A. de Lieto Vollaro, Outdoor thermal comfort in the Mediterranean area. A transversal study in Rome, Italy, *Building and Environment* 96 (2016) 46-61.
- [30] K. Blazejczyk, Y. Epstein, G. Jendritzky, H. Staiger, B. Tinz, Comparison of UTCI to selected thermal indices, *International journal of biometeorology* 56(3) (2012) 515-535.
- [31] H. Zhang, E. Arens, C. Huizenga, T. Han, Thermal sensation and comfort models for non-uniform and transient environments, part III: Whole-body sensation and comfort, *Building and Environment* 45(2) (2010) 399-410.
- [32] H. Zhang, E. Arens, C. Huizenga, T. Han, Thermal sensation and comfort models for non-uniform and transient environments, part II: Local comfort of individual body parts, *Building and Environment* 45(2) (2010) 389-398.
- [33] X. Zhou, H. Zhang, Z. Lian, Y. Zhang, A model for predicting thermal sensation of Chinese people, *Building and Environment* 82 (2014) 237-246.
- [34] X. Zhou, H. Zhang, Z. Lian, L. Lan, Predict thermal sensation of Chinese people using a thermophysiological and comfort model, *Indoor Air* (2014).
- [35] T. Han, K.-H. Chen, B. Khalighi, A. Curran, J. Pryor, M. Hepokoski, Assessment of various environmental thermal loads on passenger thermal comfort, *SAE International Journal of Passenger Cars-Mechanical Systems* 3(2010-01-1205) (2010) 830-841.
- [36] A. Alahmer, M. Omar, A.R. Mayyas, A. Qattawi, Analysis of vehicular cabins' thermal sensation and comfort state, under relative humidity and temperature control, using Berkeley and Fanger models, *Building and environment* 48 (2012) 146-163.
- [37] N. Gao, H. Zhang, J. Niu, Investigating indoor air quality and thermal comfort using a numerical thermal manikin, *Indoor and built environment* 16(1) (2007) 7-17.
- [38] A. Standard, Standard 55-2010: "Thermal Environmental Conditions for Human Occupancy"; ASHRAE, Atlanta USA (2010).
- [39] J.R. Howell, M.P. Menguc, R. Siegel, Thermal radiation heat transfer, CRC press 2010.
- [40] R.J. de Dear, E. Arens, Z. Hui, M. Oguro, Convective and radiative heat transfer coefficients for individual human body segments, *International Journal of Biometeorology* 40(3) (1997) 141-156.

- 737 [41] E.A. Arens, H. Zhang, The skin's role in human thermoregulation and comfort, Center for the  
738 Built Environment (2006).
- 739 [42] H. Zhang, Human thermal sensation and comfort in transient and non-uniform thermal  
740 environments, Center for the Built Environment (2003).
- 741 [43] A.K. Melikov, Z. Popiolek, M. Silva, I. Care, T. Sefker, Accuracy limitations for low-velocity  
742 measurements and draft assessment in rooms, HVAC&R Research 13(6) (2007) 971-986.
- 743 [44] J. Van Hoof, Forty years of Fanger's model of thermal comfort: comfort for all?, Indoor air  
744 18(3) (2008) 182-201.
- 745